Chemical Science

RSCPublishing

ARTICLE

Dark to Light! A New Strategy for Large Stokes Shift Dyes: Coupling of Dark Donor with Tunable High Quantum Yield Acceptors

Dongdong Su,[a] Juwon Oh,[c] Sung-Chan Lee,[b] Jong Min Lim,[c] Srikanta Sahu,[b] Xiaotong Yu,[a] Dongho Kim*[c] and Young-Tae Chang*[a,b]

A new strategy, for constructing large Stokes shift dyes by coupling low quantum yield (less than 1%) BODIPY donor (**BDN**) with tunable high quantum yield BODIPY acceptors (**BDM**), has been explored to synthesize a set of novel BODIPY-based resonance energy transfer (RET) dyes, named **BNM**. The low quantum yield of donor is ascribed to the intramolecular rotation of the phenyl rings, which has been proved by controlling the viscosity and temperature of solvent. However, upon excitation of **BNM** compounds at the donor absorption wavelength, the tunable emissions from 560 nm to 617 nm were obtained, with a high quantum yield of up to 0.75. Ultrafast dynamic study demonstrated that the absorbed energy was transferred to the acceptor (**BDM**) with a high energy transfer rate before being quenched by non-radiative intramolecular rotations. Using dark donor makes it possible to avoid fluorescence leaks from donor emission. This is the new set of RET dyes which can be excited by low quantum yield donor to emit a tunable wide range of high fluorescence emission.

Introduction

Fluorescent molecules have been successfully applied in various bioimaging and medicinal applications for several decades due to their high sensitivity and easy visibility.[1-5] Multiplexing,[6-8] by which multiple fluorophore signals are combined into one single experiment, is well developed in the fields of DNA sequencing labeling,[9, 10] multicolor labeling of individual cells[11] and multispectral labeling of proteins.[6, 12] The multicolor fluorescent labeling approach, which exhibits the advantage of time resolved labeling, is hampered by the limited candidates of multicolor fluorescent molecules.

Single fluorophore based libraries could show tunable emission by changing building blocks on core skeletons, such Seoul-Fluor,[13] **BDD**[14] and **BDM**.[15] However, their prospect for single excitation techniques, such as high-throughput screening or multiplexing, is not ideal. And it is difficult to find one single wavelength excitation suitable for all fluorophores in these libraries due to their tunable emission. If excited by single wavelength light, the fluorescence intensities of dyes, which emit at longer wavelengths, will be diminished due to less effective energy absorption at the excitation wavelength.[16]

Theoretically, the above mentioned problems can be solved by Förster resonance energy transfer (FRET) strategy.[17] FRET-based libraries constructed with the same donor but different acceptors allow us to excite the donor fluorophore with one single wavelength excitation and obtain tunable emissions according to different acceptors.[18, 19] Traditionally, dyes with high extinction coefficient and high quantum yield such as coumarin,[20, 21] BODIPY,[22, 23] rhodamine[24, 25] are chosen as donor for FRET strategy. However, using a high quantum yield

dye as a donor will lead to fluorescence leaking from the donor part due to the energy transfer efficiency or the environment changes, and this drawback may hamper their applications in biology. Furthermore, most of the reported FRET based fluorophores showed rather limited short emission wavelengths or relatively small pseudo-Stokes shifts, especially for BODIPY compounds. Burgess and coworkers developed the rational design of fluorescent labels based on through-bond energy transfer (TBET).[16, 26-30] This kind of compound shows high energy transfer rate and tunable fluorescent output through a wide emission window via cassettes composed of the same donor and different acceptors. This excellent work explored a powerful gateway for the generation of desired emission spectra. However, fluorescence leakage from the donor part still has not been overcome[29] and relatively small pseudo-Stokes shifts of some FRET-based dyes may induce self-quenching.[16, 26] In this regard, using dark donor to construct RET-based fluorescent dyads is an ideal design process.

For robust and universal applications of RET dyes, it is worthwhile to design the high quality fluorescent dyads: 1) high fluorescence intensity and tunable emission wavelength excited at one single wavelength excitation; 2) absorbance of light at high extinction coefficient and no fluorescence from donor part to insure there is no background influence; 3) large pseudo-Stokes shifts and emission shifts to avoid serious self-quenching and fluorescence detection errors caused by excitation backscattering effects,[23, 31] and 4) highly efficient energy transfer. Here, we report a new strategy for design and synthesis of a new set of BODIPY-based RET dyes (**BNM**), which use low quantum yield donor to generate high quantum

yield, tunable emission wavelengths and well resolved fluorescence.

Results and discussion

Design and synthesis

The synthetic scheme and the structures of **BNM** are shown in Scheme S1. **BDN** skeleton was chosen as donor due to the following reasons: 1) relatively high extinction coefficient, which indicates its high ability for light harvesting; 2) the maximum absorption at around 490 nm, which is accordant with widespread argon laser (488/514 nm); 3) quite low quantum yield, which can reduce fluorescence leakage from the donor part. For acceptors, we chose another type of BODIPY compounds, **BDM**, which shows different electrochemical and photochemical properties, such as tunable emission wavelength and tunable quantum yield. Cyanuric chloride was chosen as linker part due to its high stability, high reaction activity[32, 33] and good biocompatibility with various biological effects.[34-39]
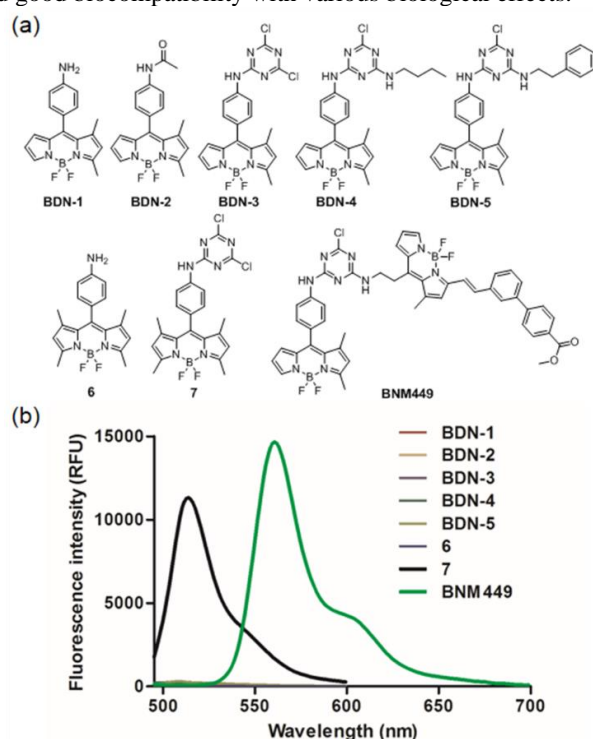

Fig. 1 (a) Structures of **BDN-1** derivatives and **BNM449**; (b) Fluorescence emission spectra of donor derivatives and **BNM449** (10 μM in EtOH, λ_{ex}= 470 nm).

General photophysical properties of BNM

The chemical diversity of the aldehyde building blocks on acceptor part gave rise to very diverse spectral properties for **BNM** (Fig. S1 and Table S1). The absorption spectra of **BNM** show two distinguished peaks corresponding to the donor and acceptor respectively, which reveals that the electronic interactions between the donor and the acceptor are very weak.[31] For all compounds, the absorption peaks related to donor part remain the same, while the acceptor related peaks change depending on the diversity of **BDM** compounds. The maximum fluorescence emission varied in the range of 560 – 617 nm based on the emission of their corresponded acceptors. Also, it was demonstrated that upon excitation of the donor (**BDN**) at 470 nm, the absorbed energy can be transferred to the acceptor (**BDM**) with high efficiency and with a high quantum

yield of up to 0.75. Also, the excitation and absorption spectra show good overlap which reinforce the perfect efficient energy transfer (Fig. S1c).[40] Both of these phenomena indicate that the RET occurs between the two fluorophores.

Rationalization of low quantum yield donor

The quantum yield of donor part **BDN-1** is quite low, while **BNM** shows high quantum yield. In order to make it clear whether the linker part influences the quantum yield of the **BDN-1**, several **BDN-1** derivatives (**BDN 2** to **5**) were designed and synthesized as control compounds (Fig. 1a). The quantum yield results show that all **BDN-1** derivatives exhibit almost no fluorescence, which means that the linker part in **BNM** does not significantly influence the quantum yield of the donor (Fig. 1b and Table S2). However, after combining with the acceptor **BDM449**, the fluorescence quantum yield of **BNM449** becomes as high as 75% (Fig. 1b). These results indicate that strong emission spectra can be generated by using low quantum yield dye as donor. It also should be noted that there is no observed fluorescence leakage from donor part, which makes it a potential fluorophore for single excitation technique. Based on all the photophysical properties, BODIPY based dyads, **BNM**, is expected to be good RET-pair with high fluorescence intensity without any fluorescence leakage.

To investigate the reason for low quantum yield of **BDN**, compounds **6** and **7** were synthesized. The fluorescence intensity of compound **7** is quite high with quantum yield of 0.57. In contrast, almost no fluorescence was observed from **BDN-3** (Fig. 1b). Comparing the structures of **BDN-3** and compound **7**, we found that the number of methyl groups on the BODIPY core structure is the mainly difference. On this basis, we speculated that the reason for low quantum yield of **BDN-3** is due to the intramolecular rotation of the phenyl rings around the axes of the single bonds linked to the BODIPY core.
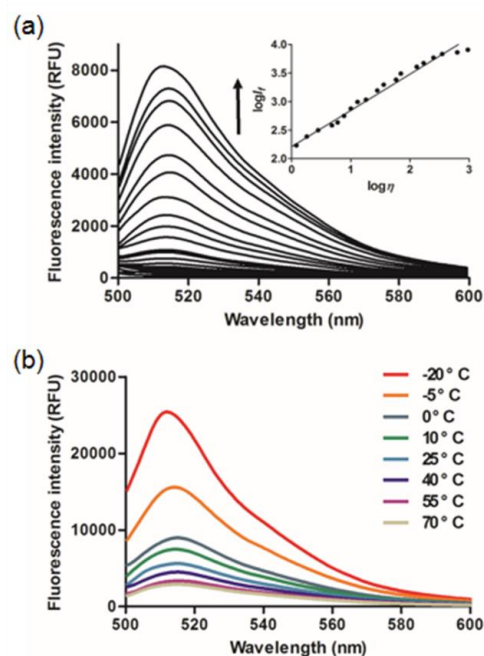

Fig. 2 (a) Changes of fluorescence spectra of **BDN-3** with the variation of solution viscosity (MeOH/glycerol system). Inset: The linearity of $\log I_f$ versus $\log \eta$ plot of **BDN-3** (10 μM, λ_{ex}= 470 nm); (b) Fluorescence spectra of **BDN-3** (10 μM, λ_{ex}= 470 nm) at different temperatures in MeOH-glycerol (30/70, v/v).

To confirm this speculation, we choose **BDN-3** as donor for further study, which can remove the influence of the photoinduced electron transfer (PET) phenomenon observed in **BDN-1**. **BDN-3** showed high extinction coefficient but low quantum yield, which means that the absorbed energy was lost through other routes rather than fluorescence. Rotational energy relaxation has been known to greatly affect emission properties by non-radiative deactivation processes.[41, 42] We suppose that the active intramolecular rotations of the phenyl rings around the axes of the single bonds linked to the BODIPY core structure may accelerate the non-radiative decay, thus making the molecule nonemissive. To prove the proposed explanation, we designed control experiments by increasing the viscosity or decreasing the temperature of solvent, which was expected to hamper the rotation of the phenyl rings and further restore the fluorescence of **BDN-3**.[43] As the viscosity increased, the fluorescence intensity of **BDN-3** was greatly enhanced by more than 100 times and the quantum yield changes from 0.01 to 0.57 (Fig. 2a). Similar to the function of high-viscous solution, lowering the temperature could also restrict the rotation of **BDN-3**.[44] The results show that the fluorescence of **BDN-3** has been dramatically influenced by the temperature of the test environment, which may control the thermally susceptible intramolecular rotations (Fig. 2b). Based on all the experimental results, it can be concluded that the low quantum yield of **BDN-3** donor is due to the intramolecular rotation of the phenyl rings, which rotate around the axes of the single bonds linked to the BODIPY core.

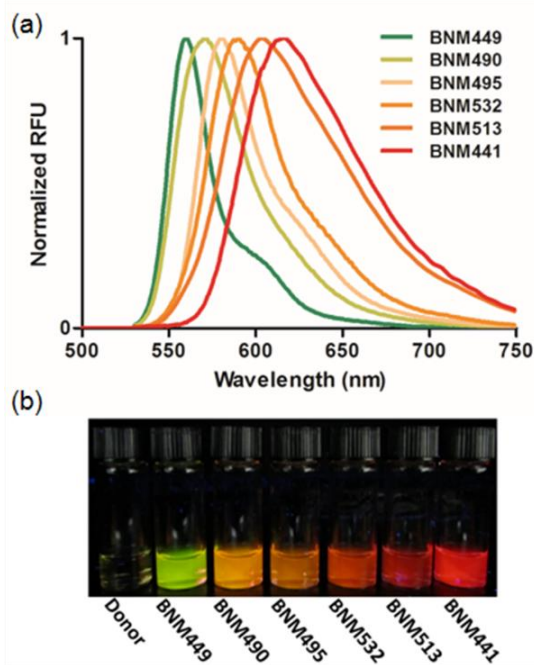**Tunable emission property**

Fig. 3 (a) The normalized fluorescence of donor only and **BNM** compounds with different maximum emission wavelength. All the emission of the **BNM** compounds were measured in EtOH (10 μM, λ_{ex}= 470 nm); (b) Pictures of donor and selected **BNM** compounds (10 μM) solutions under irradiation with a hand-held 365 nm lamp.

Besides the unique RET properties, **BNM** compounds show tunable fluorescence emission, which is one of the most

important features for fluorophore design.[13, 45] As shown in Fig. 3, when the set of **BNM** dyes are excited at 470 nm (donor band), the maximum emission changed from 560 to 617 nm with the corresponding emission color change from green to red. In other words, **BNM** can generate a broad range of the emission spectra based on single wavelength excitation. Also, the pseudo-Stokes shifts of **BNM** compounds changed from 66 to 123 nm, which contributes to the resolution for multiplexing experiments (Table S1).
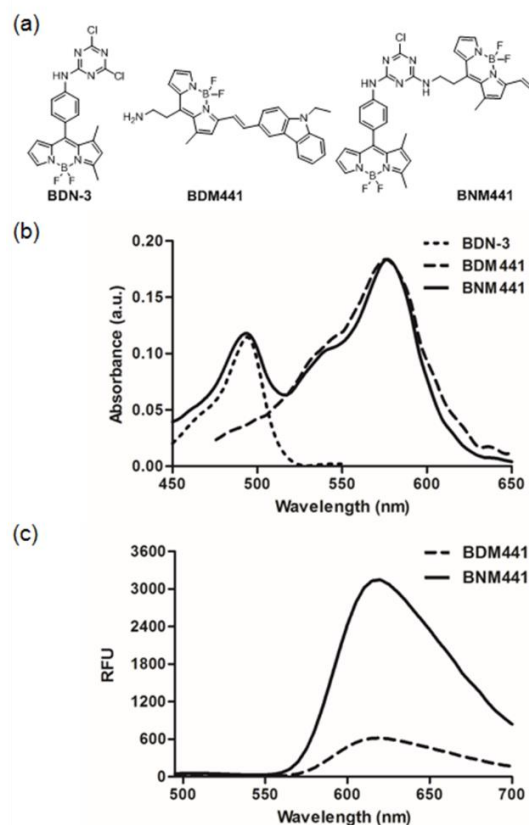

Fig. 4 (a) Structures of the donor **BDN-3**, acceptor **BDM441** and **BNM441**; (b) Absorbance and (c) Fluorescence spectra of **BDM441** and **BNM441** in EtOH (10 μM, λ_{ex}= 470 nm).

Rationalization of RET process

To exemplify and explain the photophysical properties of the **BNM** dyads, we chose **BNM441** as an example for analysis due to its high quantum yield and large Stokes shift. The structures of **BNM441**, its relative donor **BDN-3** and acceptor **BDM441** are shown in Fig. 4a. The absorption spectra of the **BNM441** displayed the characteristic absorption bands of donor **BDN-3** around 494 nm and **BDM441** around 577 nm without significant changes. Upon excitation of **BNM441** at the donor absorption band (470 nm), while only the characteristic emission band of the acceptor **BDM441** around 617 nm was observed, the emission of the donor **BDN-3** was not observed (Fig. 4c). This indicates that the majority of the non-radiative energy loss of donor was converted to the acceptor's fluorescence output with minimum leak of donor emission. Furthermore, the pseudo-Stokes shift between the absorption of donor and the emission of acceptor in **BNM** is larger than 120 nm, which is much larger than that **BDM441** itself (Table 1). The fluorescence intensity of **BNM441** is five times larger than

Table 1. Photophysical data of **BDN-3**, **BDM441** and **BNM441** in EtOH.

	λ_{abs} (nm)[a]	Log ε_{max}	λ_{abs} (nm)[b]	Log ε_{max}	λ_{em} (nm)	Φ[c]	$\Delta\lambda$[d]
BDN-3	494	4.79	–	–	511	<0.01	17
BDM441	–	–	576	4.98	614	0.45	38
BNM441	494	4.79	577	4.98	617	0.38	123

[a]The maximal absorption of the **BDN-3** part; [b]The maximal absorption of the **BDM** part; [c]Fluorescence quantum yields were measured in EtOH (10 µM, λ_{ex}= 470 nm) using rhodamine B (Φ=0.7 in EtOH) as a standard;[46] [d]Pseudo-Stokes shift of the **BNM441** and the Stokes shift of the **BDN-3** and **BDM441**.

BDM441 by photoexcitation at the same wavelength. Since the fluorescence intensity plays an important role in practical applications, the **BNM** dyads with relatively higher fluorescence intensity may attract much attention for applications.

Femtosecond transient absorption (fs-TA) measurements were carried out for better understanding of the energy transfer processes occurring in the donor-acceptor pair in EtOH (Fig. 5a and Fig. S3).[28, 47] The TA spectrum of **BDN-3** shows a combination of ground state bleaching (GSB) and stimulated emission (SE) bands at around 500 nm, which quickly decays with a time constant of 33 ps due to the intramolecular rotation of *meso*-phenyl group as observed in the viscosity and temperature control experiment (Table S3). In the case of acceptor moiety, excited-state absorption (ESA) band in the region of 450-530 nm and GSB and SE bands in 530-750 nm were observed, respectively. As a delay time increases, the SE band becomes red-shifted and broader, indicating a charge transfer (CT) behavior between BODIPY and carbazole moieties of the acceptor with a time component of 10 ps. In accordance with the fluorescence lifetime, the GSB and SE bands exhibit exponential decay profiles with a time constant of 3 ns. For the RET pair, **BNM441**, photoexcitations at 500 and 580 nm were employed as a control experiment. Interestingly, while the TA spectrum of **BNM441** by photoexcitation at 580 nm is similar to that of acceptor only, that by photoexcitation at 500 nm exhibits additional GSB and SE bands at around 500 nm, which is thought to arise from excited-state dynamics of donor (Fig. S3). As discussed in the absorption and fluorescence emission spectra, these TA spectra of **BNM441** clearly demonstrate energy transfer processes. Moreover, the TA decay profile of donor only shows a single decay component, 33 ps, but that of dyads is well-described by a much shorter time component of 1.2 ps (Fig. 5b and 5c). These results indicate that a decay time of donor, 33 ps, is significantly reduced to 1.2 ps in the RET pair, **BNM441**, which can be a clear evidence of efficient RET with a rate of k_{RET} = 8.3×10^{11} s^{-1}. The observed RET rate is well-matched with our calculation based on the intramolecular energy transfer and the RET efficiency was estimated to be 96% (Table S4).[44, 48, 49] Here, despite the low quantum yield and short excited-state lifetime of donor, the efficient RET process in **BNM441** can be attained by the large spectral overlap of RET pair and the high extinction coefficient of acceptor. Considering all the data, we can make a conclusion that the energy absorbed by the donor is transferred to the acceptor with a fast energy transfer rate before being quenched by non-radiative intramolecular rotations,[50] suggesting that highly efficient RET can be achieved through the low quantum yield of donor in **BNM441**.

Conclusions

By connecting one BODIPY donor with BODIPY acceptors, a set of BODIPY-based RET dyes was designed and synthesized. The new RET strategy allows us to obtain tunable emission wavelengths and high quantum yield by single wavelength excitation. The idea of using low quantum yield BODIPY dye as donor to reduce the fluorescence leakage from the donor part generated a new example of RET dyad. And this concept can be potentially extended to other donor-acceptor systems. The pump- probe measurement was applied to prove the probability of using low quantum yield dye as donor because of higher energy transfer rate in RET than self-quenching by non-radiative intramolecular rotations. Based on these optical properties, **BNM** compounds can be functionalized as fluorescent probes for potential fluorescence labeling in bioimaging.
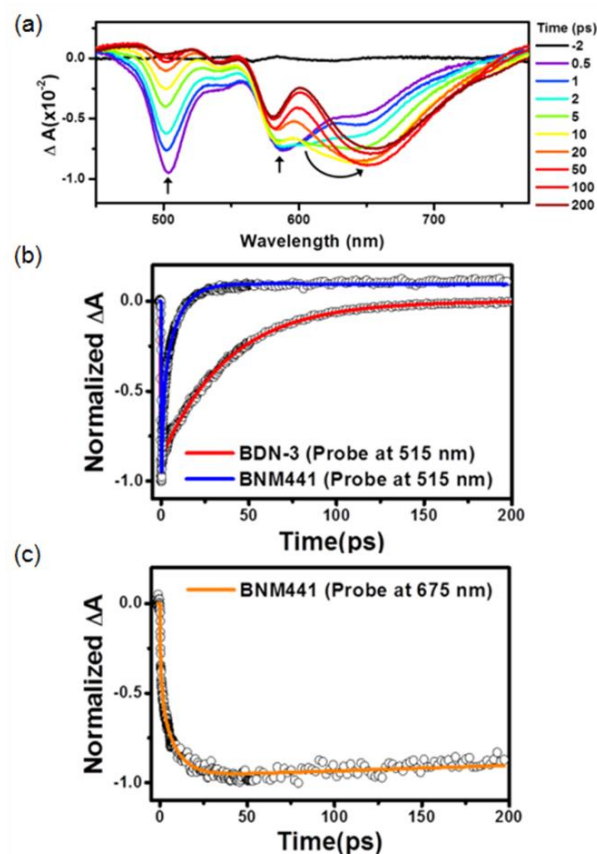

Fig. 5 (a) Transient absorption spectrum of **BNM441**; (b) The excited-state decay of donor (**BDN-3**) in the absence and presence of acceptor measured at probe wavelength of 515 nm; (c) The excited-state dynamics of acceptor in RET-pair **BNM441** measured at probe wavelength of 675 nm. The photoexcitation is at 500 nm and all data were measured in EtOH.

Acknowledgements

Experimental

Materials and methods

The chemicals, including aldehydes and solvents, were purchased from Sigma Aldrich, Fluka, MERCK, Acros and Alfa Aesar. All the chemicals were directly used without further purification. Normal phase column chromatography purification was carried using MERCK silica Gel 60 (Particle size: 230-400 mesh, 0.040-0.063 mm).

Spectroscopic and quantum yield data were measured on a SpectraMax M2 spectrophotometer (Molecular Devices). Data analysis was performed using Graph Prism 5.0.

^{1}H-NMR and ^{13}C-NMR spectra were recorded on Bruker ACF300 (300 MHz) and AMX500 (500 MHz) spectrometers, and chemical shifts are expressed in parts per million (ppm) and coupling constants are reported as a J value in Hertz (Hz). Characterization details (NMR) are contained in the Supporting Information.

Quantum Yield Measurements

Quantum yields for all the fluorescent compounds were measured by dividing the integrated emission area of their fluorescent spectrum against the area of Rhodamine B in EtOH excited at 490 nm ($\Phi_{\text{rho-B}} = 0.7$).[46] Quantum yields where then calculated using equation (1), where F represents the integrated emission area of fluorescent spectrum, η represents the refractive index of the solvent, and Abs represents absorbance at excitation wavelength selected for standards and samples. Emission was integrated from 530 nm to 750 nm.

$$\Phi_{flu}^{sample} = \Phi_{flu}^{reference} \left(\frac{F^{sample}}{F^{reference}} \right) \left(\frac{\eta^{sample}}{\eta^{reference}} \right) \left(\frac{Abs^{reference}}{Abs^{sample}} \right) \quad (1)$$

Femtosecond Transient Absorption Measurements

The femtosecond time-resolved transient absorption (fs-TA) spectrometer consisted of Optical Parametric Amplifiers (Palitra, Quantronix) pumped by a Ti:sapphire regenerative amplifier system (Integra-C, Quantronix) operating at 1 kHz repetition rate and an optical detection system. The generated OPA pulses had a pulse width of ~ 100 fs and an average power of 100 mW in the range 280-2700 nm which were used as pump pulses. White light continuum (WLC) probe pulses were generated using a sapphire window (3 mm of thickness) by focusing of small portion of the fundamental 800 nm pulses which was picked off by a quartz plate before entering to the OPA. The time delay between pump and probe beams was carefully controlled by making the pump beam travel along a variable optical delay (ILS250, Newport). Intensities of the spectrally dispersed WLC probe pulses are monitored by a High Speed spectrometer (Ultrafast Systems). To obtain the time-resolved transient absorption difference signal (DA) at a specific time, the pump pulses were chopped at 500 Hz and absorption spectra intensities were saved alternately with or without pump pulse. Typically, 4000 pulses excite samples to obtain the fs-TA spectra at a particular delay time. The polarization angle between pump and probe beam was set at the magic angle (54.7°) using a Glan-laser polarizer with a half-wave retarder in order to prevent polarization-dependent signals. Cross-correlation fwhm in pump-probe experiments was less than 200 fs and chirp of WLC probe pulses was measured to be 800 fs in the 400-800 nm region. To minimize chirp, all reflection optics in the probe beam path and the 2 mm path length of quartz cell were used. After the fluorescence and fs-TA experiments, we carefully checked absorption spectra of all compounds to detect if there were artifacts due to degradation and photo-oxidation of samples. HPLC grade solvents were used in all steady-state and time-resolved spectroscopic studies. The three-dimensional data sets of ΔA versus time and wavelength were subjected to singular value decomposition and global fitting to obtain the kinetic time constants and their associated spectra using Surface Xplorer software (Ultrafast Systems).

Time-resolved Fluorescence Measurements

Time-resolved fluorescence lifetime experiments were performed by the time-correlated single-photon-counting (TCSPC) technique. As an excitation light source, we used a Ti:sapphire laser (Mai Tai BB, Spectra-Physics) which provides a repetition rate of 800 kHz with ~ 100 fs pulses generated by a homemade pulse-picker. The output pulse of the laser was frequency-doubled by a 1 mm thickness of a second harmonic crystal (β-barium borate, BBO, CASIX). The fluorescence was collected by a microchannel plate photomultiplier (MCP-PMT, Hamamatsu, R3809U-51) with a thermoelectric cooler (Hamamatsu, C4878) connected to a TCSPC board (Becker&Hickel SPC-130). The overall instrumental response function was about 25 ps (the full width at half maximum (fwhm)). A vertically polarized pump pulse by a Glan-laser polarizer was irradiated to samples, and a sheet polarizer, set at an angle complementary to the magic angle (54.7°), was placed in the fluorescence collection path to obtain polarization-independent fluorescence decays.

Synthesis and Characterization

The **BDN-1**, **BDN-3** and **BDM** were synthesized following our previous report.[15, 51, 52] Compound **6** and **7** were synthesized following the reported method.[53]

General procedure for synthesis of **BNM** compounds

BDN-3 (1 equiv), **BDM** compound (1 equiv) and DIEA (2 equiv) were dissolved in THF and stirred at room temperature for 2 h. After evaporation of the solvent, the crude product was purified by silica gel chromatography (eluents: CH_2Cl_2 to CH_2Cl_2–MeOH (95: 5)) to afford the corresponding **BNM** set compounds as red solid.

Notes and references

[a] Department of Chemistry & MedChem Program of Life Sciences Institute, National University of Singapore, 117543, Singapore. E-mail: chmcyt@nus.edu.sg

[b] Singapore Bioimaging Consortium, Agency for Science, Technology and Research (A*STAR), 138667, Singapore

[c] Department of Chemistry and Spectroscopy of π -Functional Electronic Systems, Yonsei University, Seoul, 120-749, Korea. E-mail: dongho@yonsei.ac.kr

1. L. Zeng, E. W. Miller, A. Pralle, E. Y. Isacoff and C. J. Chang, *J. Am. Chem. Soc.*, 2006, **128**, 10-11.

2. S. C. Dodani, Q. He and C. J. Chang, *J. Am. Chem. Soc.*, 2009, **131**, 18020-18021.

3. S. C. Dodani, D. W. Domaille, C. I. Nam, E. W. Miller, L. A. Finney, S. Vogt and C. J. Chang, *Proc. Natl. Acad. Sci. USA*, 2011, **108**, 5980-5985.

4. S. C. Dodani, S. C. Leary, P. A. Cobine, D. R. Winge and C. J. Chang, *J. Am. Chem. Soc.*, 2011, **133**, 8606-8616.

5. J. Chan, S. C. Dodani and C. J. Chang, *Nat. chem.*, 2012, **4**, 973-984.

6. B. N. G. Giepmans, S. R. Adams, M. H. Ellisman and R. Y. Tsien, *Science*, 2006, **312**, 217-224.

7. R. Y. Tsien and A. Miyawaki, *Science*, 1998, **280**, 1954-1955.

8. D. C. Dieterich, *Curr. Opin. Neurobiol*, 2010, **20**, 623-630.

9. F. Samain, S. Ghosh, Y. N. Teo and E. T. Kool, *Angew. Chem. Int. Edit.*, 2010, **49**, 7025-7029.

10. Y. N. Teo, J. N. Wilson and E. T. Kool, *J. Am. Chem. Soc.*, 2009, **131**, 3923-3933.

11. J. B. Delehanty, C. E. Bradburne, K. Susumu, K. Boeneman, B. C. Mei, D. Farrell, J. B. Blanco-Canosa, P. E. Dawson, H. Mattoussi and I. L. Medintz, *J. Am. Chem. Soc.*, 2011, **133**, 10482-10489.

12. V. Singh, S. Wang and E. T. Kool, *J. Am. Chem. Soc.*, 2013, **135**, 6184-6191.

13. E. Kim, M. Koh, B. J. Lim and S. B. Park, *J. Am. Chem. Soc.*, 2011, **133**, 6642-6649.

14. D. T. Zhai, S. C. Lee, M. Vendrell, L. P. Leong and Y. T. Chang, *Acs Comb. Sci.*, 2012, **14**, 81-84.

15. M. Vendrell, G. G. Krishna, K. K. Ghosh, D. T. Zhai, J. S. Lee, Q. Zhu, Y. H. Yau, S. G. Shochat, H. Kim, J. Chung and Y. T. Chang, *Chem. Commun.*, 2011, **47**, 8424-8426.

16. G. S. Jiao, L. H. Thoresen and K. Burgess, *J. Am. Chem. Soc.*, 2003, **125**, 14668-14669.

17. J. Fan, M. Hu, P. Zhan and X. Peng, *Chem. Soc. Rev.*, 2013, **42**, 29-43.

18. T. Komatsu, K. Kikuchi, H. Takakusa, K. Hanaoka, T. Ueno, M. Kamiya, Y. Urano and T. Nagano, *J. Am. Chem. Soc.*, 2006, **128**, 15946-15947.

19. J. Yang, H. Chen, I. R. Vlahov, J. X. Cheng and P. S. Low, *Proc. Natl. Acad. Sci. USA*, 2006, **103**, 13872-13877.

20. H. Takakusa, K. Kikuchi, Y. Urano, S. Sakamoto, K. Yamaguchi and T. Nagano, *J. Am. Chem. Soc.*, 2002, **124**, 1653-1657.

21. A. E. Albers, V. S. Okreglak and C. J. Chang, *J. Am. Chem. Soc.*, 2006, **128**, 9640-9641.

22. H. B. Yu, Y. Xiao, H. Y. Guo and X. H. Qian, *Chem-Eur J.*, 2011, **17**, 3179-3191.

23. X. L. Zhang, Y. Xiao and X. H. Qian, *Angew. Chem. Int. Edit.*, 2008, **47**, 8025-8029.

24. A. Dietrich, V. Buschmann, C. Muller and M. Sauer, *J. Biotechnol.*, 2002, **82**, 211-231.

25. S. Takahashi, W. Piao, Y. Matsumura, T. Komatsu, T. Ueno, T. Terai, T. Kamachi, M. Kohno, T. Nagano and K. Hanaoka, *J. Am. Chem. Soc.*, 2012, **134**, 19588-19591.

26. R. Bandichhor, A. D. Petrescu, A. Vespa, A. B. Kier, F. Schroeder and K. Burgess, *J. Am. Chem. Soc.*, 2006, **128**, 10688-10689.

27. J. Y. Han, J. Jose, E. Mei and K. Burgess, *Angew. Chem. Int. Edit.*, 2007, **46**, 1684-1687.

28. T. G. Kim, J. C. Castro, A. Loudet, J. G. S. Jiao, R. M. Hochstrasser, K. Burgess and M. R. Topp, *J. Phys. Chem. A*, 2006, **110**, 20-27.

29. Y. Ueno, J. Jose, A. Loudet, C. Perez-Bolivar, P. Anzenbacher and K. Burgess, *J. Am. Chem. Soc.*, 2011, **133**, 51-55.

30. C. W. Wan, A. Burghart, J. Chen, F. Bergstrom, L. B. A. Johansson, M. F. Wolford, T. G. Kim, M. R. Topp, R. M. Hochstrasser and K. Burgess, *Chem-Eur J.*, 2003, **9**, 4430-4441.

31. W. Y. Lin, L. Yuan, Z. M. Cao, Y. M. Feng and J. Z. Song, *Angew. Chem. Int. Edit.*, 2010, **49**, 375-379.

32. J. T. Bork, J. W. Lee, S. M. Khersonsky, H. S. Moon and Y. T. Chang, *Org. Lett.*, 2003, **5**, 117-120.

33. J. T. Bork, J. W. Lee and Y. T. Chang, *Tetrahedron Lett.*, 2003, **44**, 6141-6144.

34. C. H. Zhou, J. K. Min, Z. G. Liu, A. Young, H. Deshazer, T. Gao, Y. T. Chang and N. R. Kallenbach, *Bioorg. Med. Chem. Lett.*, 2008, **18**, 1308-1311.

35. H. P. Harding, Y. H. Zhang, S. Khersonsky, S. Marciniak, D. Scheuner, R. J. Kaufman, N. Javitt, Y. T. Chang and D. Ron, *Cell Metab.*, 2005, **2**, 361-371.

36. D. W. Jung, D. Williams, S. M. Khersonsky, T. W. Kang, N. Heidary, Y. T. Chang and S. J. Orlow, *Mol Biosyst*, 2005, **1**, 85-92.

37. D. Williams, D. W. Jung, S. M. Khersonsky, N. Heidary, Y. T. Chang and S. J. Orlow, *Chem. Biol.*, 2004, **11**, 1251-1259.

38. J. Min, Y. K. Kim, P. G. Cipriani, M. Kang, S. M. Khersonsky, D. P. Walsh, J. Y. Lee, S. Niessen, J. R. Yates, K. Gunsalus, F. Piano and Y. T. Chang, *Nat. Chem. Biol.*, 2007, **3**, 55-59.

39. J. R. Snyder, A. Hall, L. Ni-Komatsu, S. M. Khersonsky, Y. T. Chang and S. J. Orlow, *Chem. Biol.*, 2005, **12**, 477-484.

40. H. Sunahara, Y. Urano, H. Kojima and T. Nagano, *J. Am. Chem. Soc.*, 2007, **129**, 5597-5604.

41. S. L. Gilat, A. Adronov, and J. M. J. Frechet, *Angew. Chem. Int. Edit.*, 1999, **38**, 1422-1427.

42. K. Yamada, T. Toyota, K. Takakura, M. Ishimaru and T. Sugawara, *New. J. Chem.*, 2001, **25**, 667-669.

43. J. Chen, C. C. W. Law, J. W. Y. Lam, Y. Dong, S. M. F. Lo, I. D. Williams, D. Zhu and B. Z. Tang, *Chem. Mater.*, 2003, **15**, 1535-1546.

44. X. Peng, Z. Yang, J. Wang, J. Fan, Y. He, F. Song, B. Wang, S. Sun, J. Qu, J. Qi and M. Yan, *J. Am. Chem. Soc.*, 2011, **133**, 6626-6635.

45. K. Umezawa, Y. Nakamura, H. Makino, D. Citterio and K. Suzuki, *J. Am. Chem. Soc.*, 2008, **130**, 1550-1551.

46. F. L. Arbeloa, P. R. Ojeda and I. L. Arbeloa, *J. Lumin.*, 1989, **44**, 105-112.

47. H. Langhals, A. J. Esterbauer, A. Walter, E. Riedle and I. Pugliesi, *J. Am. Chem. Soc.*, 2010, **132**, 16777-16782.

48. T, Förster, *Ann. Phys.*, 1948, **2**, 55-75.

49. T. Forster, *Discuss. Faraday. Soc.*, 1959, **27**, 7-17.

50. S. Erbas-Cakmak, O. A. Bozdemir, Y. Cakmak and E. U. Akkaya, *Chem. Sci.*, 2013, **4**, 858-862.

51. N. Y. Kang, S. C. Lee, S. J. Park, H. H. Ha, S. W. Yun, E. Kostromina, N. Gustavsson, Y. Ali, Y. Chandran, H. S. Chun, M.

Bae, J. H. Ahn, W. Han, G. K. Radda and Y. T. Chang, *Angew. Chem. Int. Edit.*, 2013, **52**, 8557-8560.

52. D. Su, C. L. Teoh, S. Sahu, R. K. Das and Y.-T. Chang, *Biomaterials*, 2014, **35**, 6078-6085.

53. T. Lazarides, G. Charalambidis, A. Vuillamy, M. Reglier, E. Klontzas, G. Froudakis, S. Kuhri, D. M. Guldi and A. G. Coutsolelos, *Inorg. Chem.*, 2011, **50**, 8926-8936.

TOC
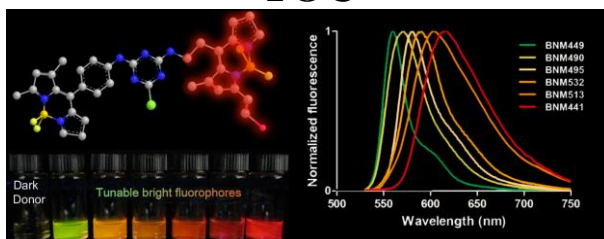
A new set of RET dyes constructed with dark donor was designed and investigated by feasibility analysis and theoretical explanation.

Supporting Information

Dark to Light! A New Strategy for Large Stokes Shift Dyes: Coupling of Dark Donor with Tunable High Quantum Yield Acceptors

Dongdong Su,[a] Juwon Oh[c], Sung-Chan Lee,[b] Jong Min Lim[c], Srikanta Sahu,[b] Xiaotong Yu[a], Dongho Kim*[,c] and Young-Tae Chang*[,a, b]

[a]Department of Chemistry and MedChem Program, Life Sciences Institute, National University of Singapore, 3 Science Drive 3, Singapore, 117543;

[b]Laboratory of Bioimaging Probe Development, Singapore Bioimaging Consortium (SBIC), 11 Biopolis Way, #02-02 Helios, Agency for Science, Technology and Research (A*STAR), Biopolis, Singapore, 138667;
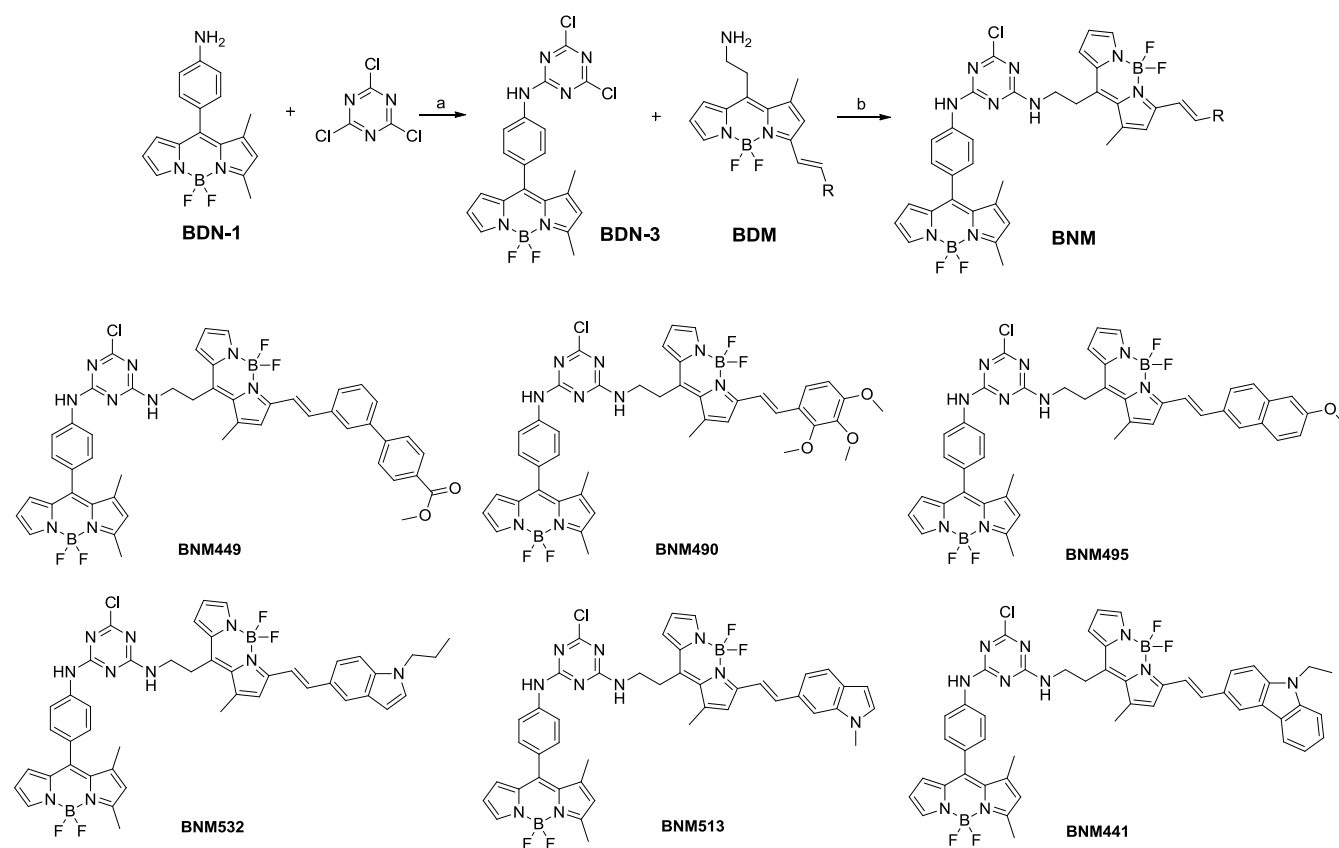
[c]Department of Chemistry and Spectroscopy of π-Functional Electronic Systems, Yonsei University, Seoul, 120-749, Korea.

List of Contents

List of contents:

9. Material and Method.

10. Synthesis and Characterizations of **BDN** derivatives and selected **BNM** compounds.

Scheme S1. Synthetic scheme and structures of **BNM** compounds[a]

[a]Reagents and conditions: (a) DIEA, THF, 0 °C., 1 h; (b) DIEA, THF, rt, 2 h.

(a)

(b)

(c)

BNM449

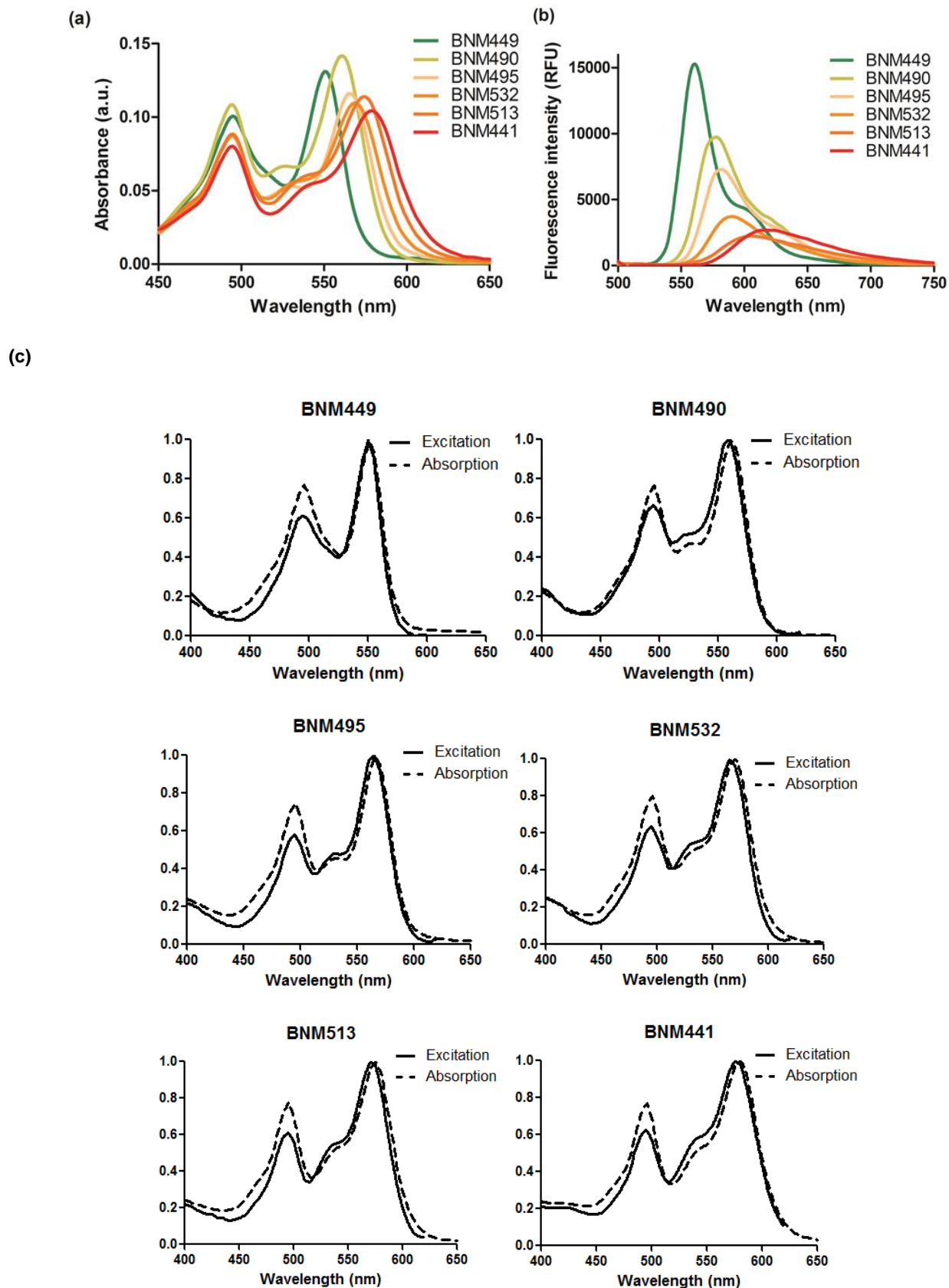BNM490

BNM495

BNM532

BNM513

BNM441

Figure S1. Spectroscopic properties of **BNM** compounds. Absorbance (a), fluorescence spectra (b) and excitation spectra (the emission wavelength was fixed at 680 nm) (c) of the selected **BNM** compounds (10 μM in EtOH, λ_{ex}= 470 nm).

Table S1. Photophysical data of **BNM** compounds.

	λ_{abs} (nm)	Log ε_{max}[a]	λ_{em} (nm)	Φ[b]	$\Delta\lambda$[c]
BNM449	494/549	4.93	560	0.75	66
BNM490	494/554	4.89	570	0.55	76
BNM495	494/563	4.99	580	0.63	86
BNM532	494/566	4.96	590	0.40	96
BNM513	494/572	4.94	603	0.30	109
BNM441	494/577	4.98	617	0.38	123

[a]The maximal absorption of the **BDM** part; [b]Fluorescence quantum yields were measured in EtOH (10 μM, λ_{ex}= 470 nm) using rhodamine B (Φ=0.7 in EtOH) as a standard. [c]Pseudo-Stokes shifts of the selected **BNM** compounds.

Table S2. The quantum yield of the **BDN** derivatives.

BDN Donor derivatives

Compound code	**BDN-1**	**BDN-2**	**BDN-3**	**BDN-4**	**BDN-5**	**BNM449**
Quantum yield[a]	0.00084	0.012	0.0085	0.010	0.0036	0.75

[a]Fluorescence quantum yields were measured in EtOH (10 μM, λ_{ex}= 470 nm) using rhodamine B (Φ=0.7 in EtOH) as a standard.

Note: For femtosecond transient absorption measurements and picosecond time-resolved fluorescence measurements, we use **BDM441-Tri** instead of **BDM441** because of its much better stability than free amine version of **BDM441**. The absorption and emission spectra show no difference in the range of 450 nm to 750 nm when tested in EtOH. The structure and spectra can be seen in the following.

BDM441

BDM441-Tri

(a)

(b)
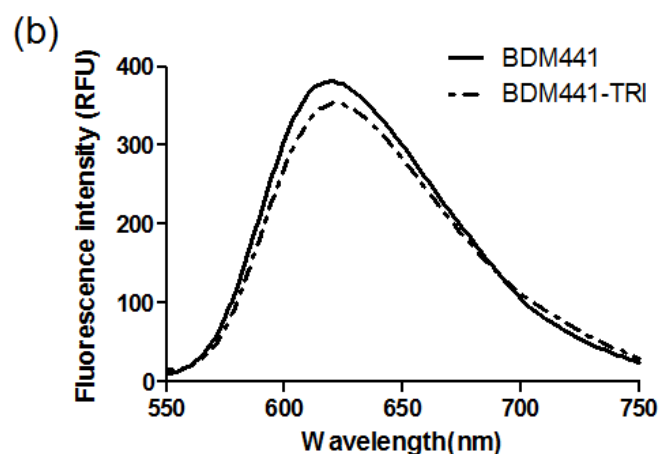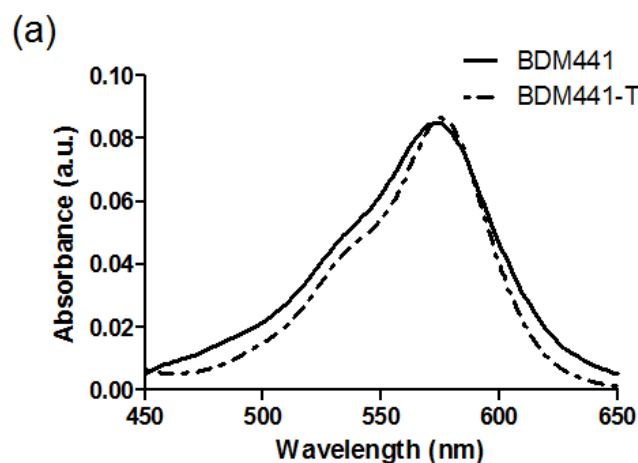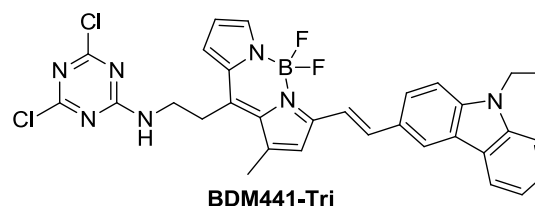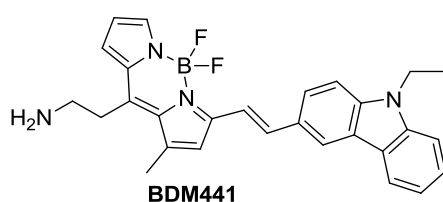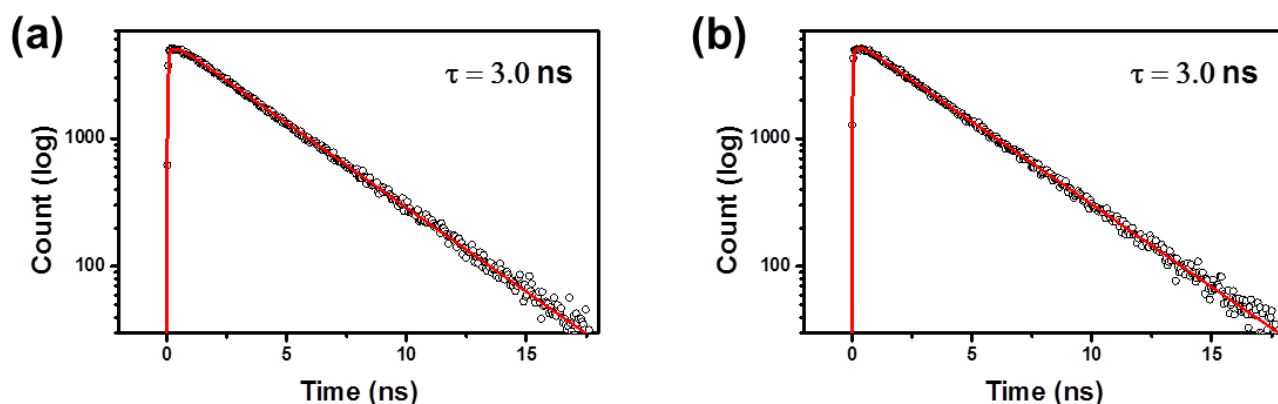
Figure S2. The fluorescence decay profiles of (a) **BDM441-Tri** and (b) **BNM441** in EtOH. The decay profiles are obtained by photoexcitation at 460 nm and monitoring at 650 nm with the time-correlated single photon counting (TSCPC) technique.

Figure S3. The fs-TA spectra (left) and decay profile (right) of (a) **BDN-3**, (b) **BDM441-Tri** and (c) **BNM441** in EtOH. The 500 nm photoexcitation is employed for **BDN-3** and 580nm for **BDM441-Tri** and **BNM441**. The ns time constants were obtained by the fluorescence lifetime based on the time-correlated single photon counting (TSCPC) technique.

Table S3. List of lifetime of **BDN-3**, **BDM441-Tri** and **BNM441**.

	BDN-3	BDM441-Tri	BNM441[a]	BNM441[b]
τ (%)	33 ps	10 ps 3.0 ns	1.2 ps 10 ps 3.0 ns[c]	10 ps 3.0 ns[c]

[a]The time component obtained by the TA decay profile by photoexcitation at 500 nm and monitoring at 515 and 675 nm; [b]The time component obtained 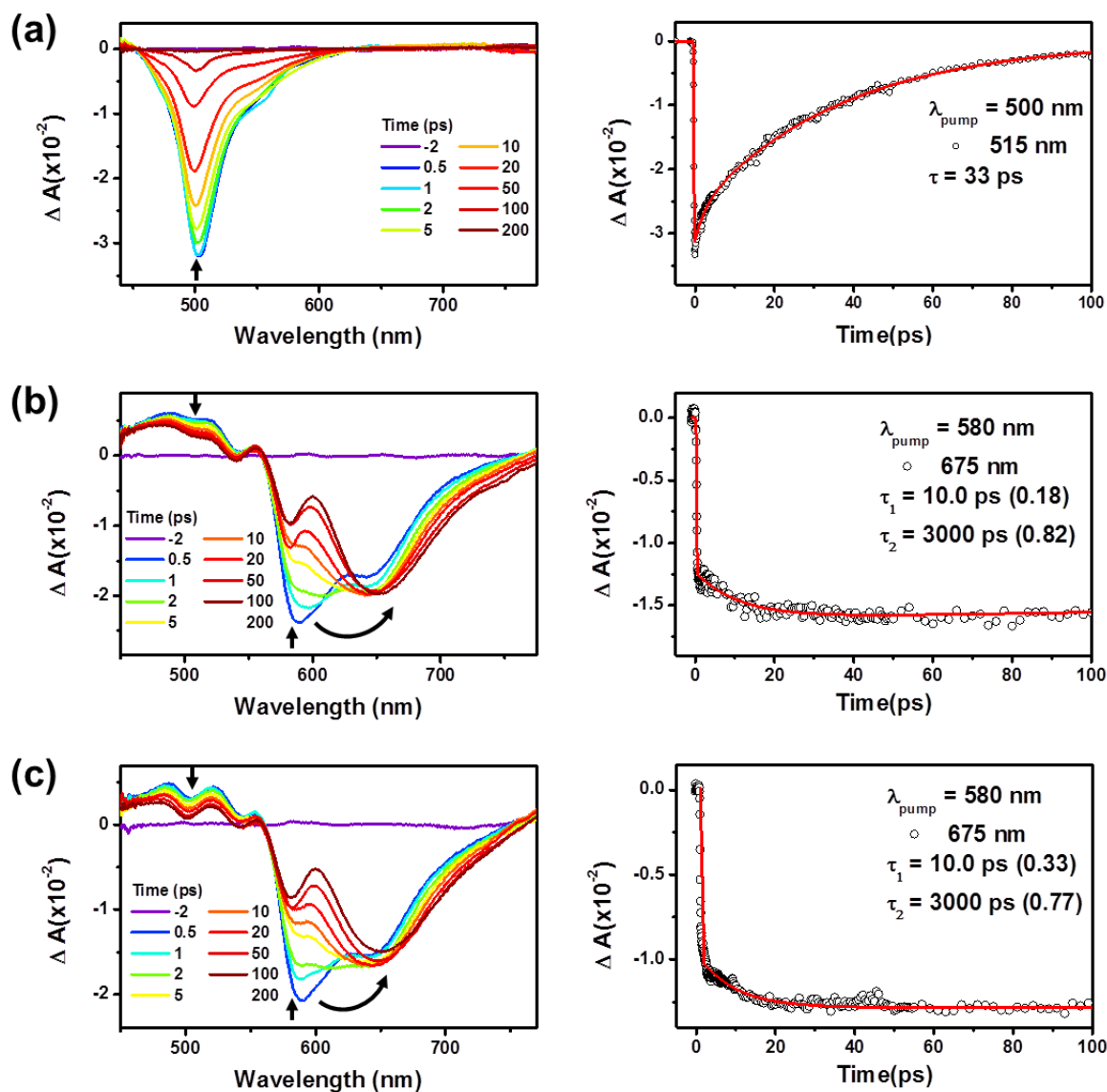by the TA decay profile by photoexcitation at 580 nm and monitoring at 675 nm; [c]The time component obtained by the fluorescence lifetime based on the time-correlated single photon counting (TSCPC) technique.

Table S4. List of parameters for Förster-type energy transfer rate and efficiency calculation.

	k_F[a]	J ($\times 10^{15} M^{-1} cm^{-1} nm^4$)[b]	κ[c]	r[d] (Å)	n[e]	Eff_{FRET}[f]
BNM441	$1.8 \times 10^{11 \sim}$ $5.0 \times 10^{12} s^{-1}$	1.477	2/3	10 ~ 18	1.36	0.96

[a]The value obtained by Forster-type energy transfer rate calculation equation $k_F = \frac{8.79 \times 10^{-5} J \kappa^2 \Phi_D}{n^4 R(\text{Å}) \tau_D}$; [b]Spectral overlap value estimated by $J = \int F(\lambda)\varepsilon(\lambda)\lambda^4 d\lambda$; [c]Orientation factor which is chosen as randomized value, 2/3, based on non-rigid molecular structure of **BNM441**; [d]Maximum and minimum intermolecular distance between donor and acceptor in **BNM441**; [e]Refractive index of EtOH; [f]RET efficiency is calculated with equation, $Eff_{RET} = k_{RET}/(k_{RET}+k_D)$, where k_D is the excited-state decay rate of donor.

Synthesis and Characterization

Synthesis of the **BDN** derivatives

Synthesis of **BDN-1**: The synthesis of **BDN-1** was following the reported literature.[1]

^{1}H-NMR (300 MHz, CDCl$_3$): δ 7.65 (s, 1H), 7.13 (d, J = 8.3 Hz, 2H), 6.75 (d, J = 8.3, 2H), 6.52 (d, J = 3.2 Hz, 1H), 6.37 (d, J = 1.8 Hz, 1H), 6.12 (s, 1H), 2.61 (s, 3H), 1.67 (s, 3H); ^{13}C-NMR (75.5 MHz, CDCl$_3$): 161.00, 147.64, 146.70, 144.44, 138.02, 135.01, 133.69, 130.39,126.92, 123.77, 122.88, 115.74, 114.57, 15.43, 15.03.

HRMS m/z (C17H16BF2N3) calculated: 311.1405, found: 334.1313 (M+Na).

BDN-1   +   DIEA / DCM → **BDN-2**
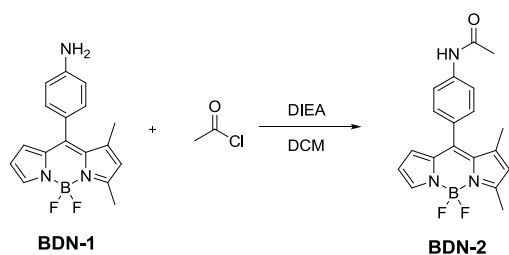
Synthesis of **BDN-2**: A solution of **BDN-1** (20 mg, 0.064 mmol) and DIEA (12 µL, 0.096 mmol) in CH$_2$Cl$_2$ (6 mL) was stirred under N$_2$ atmosphere at 0 ℃. Acetyl chloride (6 µL, 0.077 mmol) in CH$_2$Cl$_2$ (1 mL) was added dropwise and the resulting mixture was stirred at 0 ℃ for 1 h. After removal of the CH$_2$Cl$_2$, the residue was purified by silica gel chromatography (CH$_2$Cl$_2$–MeOH, 95: 5) to give **BDN-2** as a yellow solid (18 mg, 80%).

^{1}H NMR (300 MHz, CDCl$_3$): δ 7.70 (s, 1H), 7.69 (d, J=8.7 Hz, 2H), 7.34 (d, J=8.5 Hz, 2H), 7.30 (s, 1H), 6.45 (s, 1H), 6.41 (s, 1H), 6.17 (s, 1H), 2.66 (s, 3H), 2.26 (s, 3H), 1.63 (s, 3H); ^{13}C NMR (75.5 MHz, CDCl$_3$): 161.94, 160.00, 146.85, 139.20, 138.58, 134.71, 129.66, 129.46, 126.95, 123.21, 119.19, 116.01, 24.65, 15.23, 15.11.
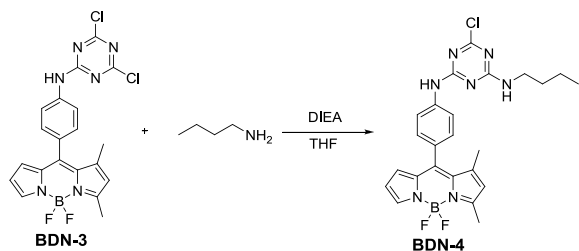
HRMS m/z (C19H18BF2N3O) calculated: 353.1511, found: 376.1418 (M+Na).

Synthesis of **BDN-4**: A solution of **BDN-3** (25 mg, 0.054 mmol) and DIEA (10 μL, 0.081 mmol) in THF (6 mL) was stirred under N_2 atmosphere at rt. 1-Butanamine (8 μL, 0.081 mmol) was added and the resulting mixture was stirred at rt for 2 h. After removal of the THF, the residue was purified by silica gel chromatography (CH_2Cl_2–MeOH, 95: 5) to give BDN-4 as a yellow solid (22 mg, 82%).

^{1}H NMR (300 MHz, CDCl3): δ 7.80 (d, J=8.5 Hz, 2H,), 7.72 (s, 1H), 7.38 (d, J=8.5 Hz, 2H), 6.49 (s, 1H), 6.42 (s, 1H), 6.18 (s, 1H), 3.57-3.47 (m, 2H), 2.67 (s, 3H), 1.66 (m, 5H), 1.49-1.41(dd, 2H), 1.03-0.97 (m, 3H); ^{13}C NMR (75.5 MHz, CDCl3): 163.84, 161.98, 146.72, 142.86, 139.14, 138.67, 134.73, 133.62, 129.66, 129.22, 126.96, 123.25, 119.78, 116.06, 41.15, 31.19, 20.00, 15.27, 15.13, 13.69.

HRMS m/z (C24H25BClF2N7) calculated: 495.1921, found: 518.1837 (M+Na).
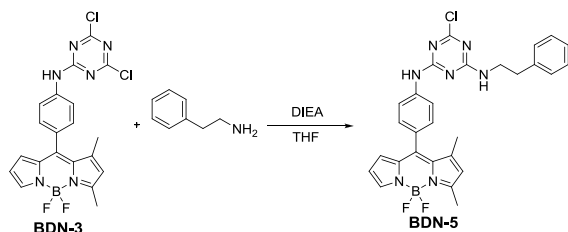
Synthesis of **BDN-5**: Compound **BDN-5** was synthesized as for **BDN-4** and obtained as a yellow solid (61%).

^{1}H NMR (300 MHz, CDCl3): δ 7.80 (d, J=8.5Hz, 2H), 7.74 (s, 1H), 7.41-7.24 (m, 7H), 6.50 (s, 1H), 6.43 (s, 1H), 6.18 (s, 1H), 3.85-3.76 (m, 2H), 2.99 (t, J=7.0Hz, 2H), 2.68 (s, 3H), 1.66(s, 3H); ^{13}C NMR (75.5 MHz, CDCl3): 169.31, 163.81, 162.03, 146.73, 139.06, 138.70, 138.07, 134.73, 129.71, 129.34, 128.81, 128.73, 128.65, 126.98, 126.95, 126.83, 123.26, 119.88, 119.80, 116.11, 42.61, 35.43, 15.28, 15.14.

HRMS m/z (C28H25BClF2N7) calculated: 543.1921, found: 542.1876 (M-H).

Synthesis of **BDM441**: The synthesis of **BDM441** was following the reported literature.[2]
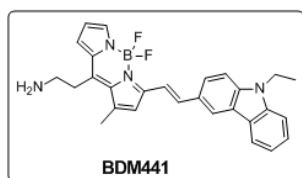
^{1}H NMR (500 MHz, CDCl$_3$-MeOD): δ 8.26 (s, 1H), 8.10 (d, J=7.2 Hz, 1H), 7.73 (d, J=7.6 Hz, 1H), 7.62 (s, 1H), 7.61 (d, J=12.3 Hz, 2H), 7.45 (s, 1H), 7.41-7.36 (m, 2H), 7.32 (s, 1H), 7.25 (s, 1H), 6.87 (s, 1H), 6.48 (s, 1H), 4.50 (s, 2H), 3.39 (s, 2H), 2.52 (s, 3H), 1.41(s, 2H), 1.24(s, 3H); ^{13}C NMR (125 MHz, CDCl$_3$-MeOD): 159.16, 144.20, 142.85, 142.84, 140.95, 140.10, 135.94, 135.12, 133.31, 126.49, 125.94, 125.63, 123.14, 122.44, 121.80, 120.83, 120.20, 120.15, 119.32, 115.37, 114.44, 108.67, 108.58, 40.53, 37.29, 26.45, 15.75, 13.26.

HRMS m/z (C28H27BF2N4) calculated: 468.2297, found: 491.2201 (M+Na).
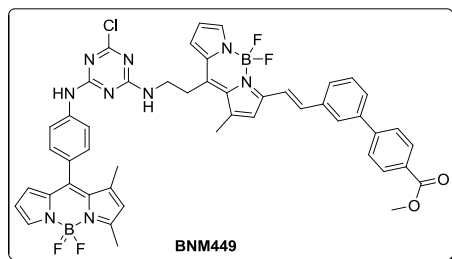
^{1}H NMR (500 MHz, CDCl$_3$): δ 8.14 (t, J=7.8 Hz, 2H), 7.80-7.58 (m, 10H), 7.52-7.40 (m, 2H), 7.33-7.29 (m, 2H), 7.06 (s, 1H), 6.79 (d, J=16.9 Hz, 1H), 6.51-6.39 (m, 3H), 6.13 (d, J=25.4 Hz, 1H), 3.97 (d, J=7.0 Hz, 3H), 3.90 (s, 1H), 3.76 (s, 1H), 3.32 (dd, J=14.2, 7.4 Hz, 2H), 2.65-2.52 (m, 6H), 1.60 (d, J=20.1 Hz, 3H); ^{13}C NMR (125 MHz, CDCl$_3$): 166.92, 166.90, 162.19, 156.74, 146.71, 144.85, 144.73, 144.17, 140.78, 140.69, 139.30, 138.74, 138.65, 138.44, 136.47, 136.35, 135.18, 134.62, 134.55, 134.47, 133.56, 130.18, 129.75, 129.51, 129.25, 128.70, 127.26, 127.10, 127.05, 126.77, 126.66, 124.11, 123.94, 123.36, 120.28, 119.92, 119.79, 119.07, 118.87, 116.40, 116.13, 52.16, 43.10, 42.59, 16.69, 16.53, 15.31.

HRMS m/z (C48H40B2ClF4N9O2) calculated: 907.3116, found: 930.3010 (M+Na).
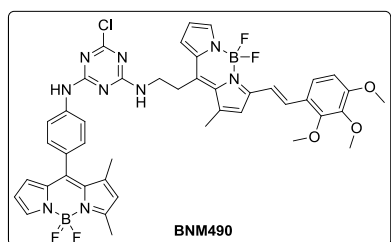
^{1}H NMR (500 MHz, CDCl$_3$): δ 7.74-7.70 (m, 3H), 7.67-7.64 (m, 2H), 7.59 (s, 1H), 7.42 (dd, J=39.8, 8.9 Hz, 1H), 7.32-7.31 (m, 2H), 7.25 (d, J=3.8 Hz, 1H), 7.02 (s, 1H), 6.81 (d, J=18.8 Hz, 1H), 6.70 (dd, J=27.4, 8.9 Hz, 1H), 6.48-6.39 (m, 3H), 6.14 (d, J=10.8 Hz, 1H), 3.98-3.88 (m, 10H), 3.77 (dd, J=13.5, 6.5 Hz, 1H), 3.31 (dd, J=14.2, 7.3 Hz, 2H), 2.64-2.51 (m, 6H), 1.61 (d, J=13.3 Hz, 3H); ^{13}C NMR (125 MHz, CDCl$_3$): 165.08, 163.37, 162.11, 158.56, 158.36, 155.52, 155.49, 152.85, 146.74, 144.35, 143.71, 142.67, 142.27, 138.64, 137.04, 135.41, 135.11, 134.91, 134.62, 134.15, 133.54, 129.71, 129.67, 126.97,

123.33, 122.84, 122.70, 120.24, 117.32, 116.10, 115.76, 107.87, 61.57, 60.89, 56.09, 43.08, 42.64, 16.64, 16.52, 15.30.

HRMS m/z ($C_{43}H_{40}B_2ClF_4N_9O_3$) calculated: 863.3065, found: 886.2998 (M+Na).
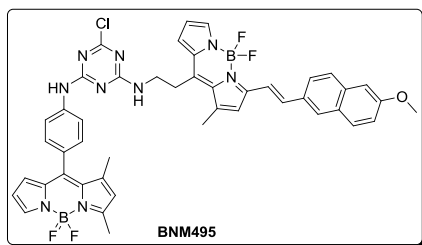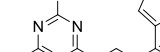
^{1}H NMR (500 MHz, CDCl$_3$): δ 7.87 (d, J=29.2 Hz, 1H),7.80-7.64 (m, 7H), 7.50 (d, J=16.1 Hz, 1H), 7.35 (d, J=8.2 Hz, 1H), 7.32 (d, J=8.3 Hz, 1H), 7.27 (d, J=3.7 Hz, 1H), 7.20-7.13 (m, 2H), 7.05 (s, 1H), 6.81 (s, 1H), 6.51-6.37 (m, 3H), 6.11 (d, J=48.0 Hz, 1H), 3.96 (d, J=8.6 Hz, 3H), 3.90 (d, J=6.6 Hz, 1H), 3.80 (dd, J=12.6, 6.2 Hz, 1H), 3.32 (dd, J=14.9, 7.8 Hz, 2H), 2.65-2.52 (m, 6H), 1.60 (d, J=32.8 Hz, 3H); ^{13}C NMR (125 MHz, CDCl$_3$): 162.13, 158.90, 158.88, 146.73, 144.16, 140.55, 140.39, 138.74, 138.63, 138.59, 137.64, 135.61, 134.34, 134.32, 133.60, 131.35, 131.23, 130.18, 130.14, 130.03, 129.78, 129.73, 129.15, 128.83, 127.57, 124.52, 124.38, 123.37, 123.34, 123.31, 120.18, 120.13, 120.10, 119.96, 119.47, 116.13, 116.09, 116.05, 106.13, 55.40, 43.29, 31.90, 16.75, 16.61, 15.33.

HRMS m/z ($C_{45}H_{38}B_2ClF_4N_9O$) calculated: 853.3010, found: 876.2903 (M+Na).
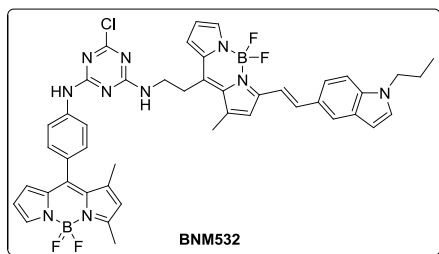
^{1}H NMR (500 MHz, CDCl$_3$): δ 7.85 (d, J=23.8 Hz, 1H), 7.73-7.46 (m, 7H), 7.37-7.30 (m, 3H), 7.20 (d, J=3.9 Hz, 1H), 7.13 (dd, J=10.0, 3.1 Hz, 1H), 6.81 (d, J=9.1 Hz, 1H), 6.54 (dd, J=10.2, 3.0 Hz, 1H), 6.46-6.38 (m, 3H), 6.12 (d, J=34.9 Hz, 1H), 4.13-4.07 (m, 2H), 3.91 (s, 1H), 3.80 (s, 1H), 3.31 (dd, J=16.0, 8.1 Hz, 2H), 3.65-2.51 (m, 6H), 1.91-1.86 (m, 2H), 1.60 (d, J=27.8 Hz, 3H), 0.96 (q, J=7.5 Hz, 3H); ^{13}C NMR (125 MHz, CDCl$_3$): 162.75, 162.17, 158.78, 146.75, 144.26, 143.11, 138.81, 138.64, 137.33, 136.48, 135.54, 135.43, 134.63, 134.00, 133.58, 130.02, 129.77, 129.72, 129.15, 128.98, 127.43, 127.33, 127.00, 126.88, 123.37, 122.62, 121.32, 120.55, 120.25, 120.12, 116.16, 116.12, 115.57, 115.50, 110.10, 102.25, 102.22, 48.25, 43.09, 31.92, 23.60, 22.67, 16.59, 14.09, 11.46.

HRMS m/z (C45H41B2ClF4N10) calculated: 854.3326, found: 877.3241(M+Na).

BNM513

^{1}H NMR (500 MHz, CDCl₃): δ 7.71-7.29 (m, 12H), 7.11 (dd, J=29.4, 2.9 Hz, 1H), 6.94 (s, 1H), 6.71 (d, J=6.2 Hz, 1H), 6.50-6.39 (m, 3H), 6.12 (d, J=34.1 Hz, 1H), 3.88 (s, 1H), 3.80 (d, J=28.1 Hz, 3H), 3.68 (s, 1H), 3.22 (s, 2H), 2.62 (d, J=29.3 Hz, 3H), 2.47 (d, J=17.6 Hz, 3H), 1.61 (d, J=21.5 Hz, 3H); ^{13}C NMR (125 MHz, CDCl₃): 165.90, 163.95, 162.00, 158.31, 146.74, 144.16, 142.86, 142.60, 142.34, 138.94, 138.86, 138.63, 138.50, 138.39, 136.95, 134.70, 134.62, 134.13, 133.58, 131.45, 131.41, 130.49, 129.73, 129.62, 129.35, 126.94, 126.81, 123.37, 123.28, 122.20, 121.19, 120.15, 120.03, 119.91, 116.04, 115.56, 101.61, 43.00, 32.98, 31.87, 22.65, 16.64, 16.51.

HRMS m/z (C43H37B2ClF4N10) calculated: 826.3013, found: 849.2920 (M+Na).

BNM441

^{1}H NMR (500 MHz, CDCl₃): δ 8.27 (d, J=25.7 Hz, 1H), 8.15 (dd, J=11.8, 7.8 Hz, 1H), 7.77-7.65 (m, 5H), 7.59-7.40 (m, 4H), 7.35-7.30 (m, 3H), 7.21 (s, 1H), 6.97 (s, 1H), 6.76 (d, J=32.1 Hz, 1H), 6.48-6.37 (m, 3H), 6.11 (d, J=45.8 Hz, 1H), 4.42-4.32 (m, 2H), 3.91 (s, 1H), 3.73 (s, 1H), 3.27 (dd, J=13.5, 6.8 Hz, 2H), 2.62 (d, J=23.7 Hz, 3H), 2.50 (s, 3H), 1.60 (d, J=27.3 Hz, 3H), 1.30-1.27 (m, 3H); ^{13}C NMR (125 MHz, CDCl₃): 163.27, 162.16, 158.49, 146.72, 144.16, 142.35, 141.21, 140.45, 138.74, 138.59, 136.41, 135.45, 134.64, 134.18, 134.04, 133.56, 129.74, 129.70, 126.97, 126.83, 126.30, 126.01, 125.96, 123.53, 123.50, 123.33, 122.87, 121.12, 120.74, 120.19, 119.74, 116.13, 116.06, 115.56, 115.47, 115.35, 115.09, 109.03, 109.00, 108.89, 108.86, 60.37, 43.00, 37.77, 29.67, 16.72, 16.53, 15.31, 13.83.

HRMS m/z (C48H41B2ClF4N10) calculated: 890.3326, found: 913.3206 (M+Na).

References

1. N. Y. Kang, S. C. Lee, S. J. Park, H. H. Ha, S. W. Yun, E. Kostromina, N. Gustavsson, Y. Ali, Y. Chandran, H. S. Chun, M. Bae, J. H. Ahn, W. Han, G. K. Radda and Y. T. Chang, *Angew. Chem. Int. Edit.*, 2013, **52**, 8557-8560.
2. M. Vendrell, G. G. Krishna, K. K. Ghosh, D. T. Zhai, J. S. Lee, Q. Zhu, Y. H. Yau, S. G. Shochat, H. Kim, J. Chung and Y. T. Chang, *Chem. Commun.*, 2011, **47**, 8424-8426.